Proc. Natl. Acad. Sci. USA
Vol. 90, pp. 9021–9025, October 1993
Cell Biology

A chromatin folding model that incorporates linker variability generates fibers resembling the native structures

(nucleosome/chromatin fiber)

C. L. WOODCOCK*, S. A. GRIGORYEV*†, R. A. HOROWITZ*, AND N. WHITAKER‡

Departments of *Biology and ‡Mathematics and Statistics, University of Massachusetts, Amherst, MA 01003

Communicated by Oscar L. Miller, Jr., July 1, 1993 (received for review March 15, 1993)

ABSTRACT **The "30-nm" chromatin fibers, as observed in eukaryotic nuclei, are considered a discrete level in a hierarchy of DNA folding. At present, there is considerable debate as to how the nucleosomes and linker DNA are organized within chromatin fibers, and a number of models have been proposed, many of which are based on helical symmetry and imply specific contacts between nucleosomes. However, when observed in nuclei or after isolation, chromatin fibers show considerable structural irregularity. In the present study, chromatin folding is considered solely in terms of the known properties of the nucleosome–linker unit, taking into account the relative rotation between consecutive nucleosomes that results from the helical twist of DNA. Model building based on this premise, and with a constant length of linker DNA between consecutive nucleosomes, results in a family of fiber- and ribbon-like structures. When the linker length between nucleosomes is allowed to vary, as occurs in nature, fibers showing the types of irregularity observed in nuclei and in isolated chromatin are created. The potential application of the model in determining the three-dimensional organization of chromatin in which nucleosome positions are known is discussed.**

The genome of most eukaryotes is complexed with proteins to form chromatin (1). Under low salt conditions *in vitro*, the complex assumes its simplest conformation and is seen as a beaded chain of 11-nm (diameter) nucleosomes (e.g., ref. 2). As the ionic strength of the medium is raised, the nucleosomal chain condenses, eventually forming a compact fiber 30–40 nm in diameter (1–3). These compact fibers observed in isolated chromatin *in vitro* are presumed to be related to similar structures seen in thin sections of certain types of nuclei such as nucleated erythrocytes (e.g., refs. 4 and 5). X-ray scattering studies of whole cells and nuclei often show 30- to 45-nm reflections that have been interpreted as arising from the center-to-center spacing of compact chromatin fibers (6). These results suggest that the compact chromatin fiber constitutes a distinct level of chromatin organization, especially for transcriptionally inactive chromatin. In this context, the architecture of the fiber would implicitly define the substrate for the regulatory events that lead to chromatin unfolding, a prerequisite for transcription.

Attempts to deduce the structure of compact chromatin fibers have resulted in a number of proposals that include both symmetrical and nonsymmetrical arrangements of nucleosomes (reviewed in ref. 7). There is evidence suggesting some degree of symmetry in fiber structure: an intermediate conformation between the nucleosome chain and the compact chromatin fiber is a "zig-zag ribbon" (2) that can display considerable regularity (8), and isolated fibers prepared for electron microscopy contain regions with a limited amount of internal order (2, 3, 9–11). All proposed model structures with symmetry are helical in nature and differ principally in the location and conformation of the linker DNA. They all predict regular nucleosome–nucleosome contacts. To date, however, insufficient evidence has been obtained to confirm any of these model structures. It has not been possible to resolve the DNA path between nucleosomes using direct microscopic observation, nor have fibers been obtained with sufficient regularity to generate diffraction patterns from which the architecture can be derived. In fact, a consistent finding of ultrastructural investigations from early studies (12) to the more recent complete three-dimensional reconstructions of sectioned and negatively stained material (reviewed in ref. 13) has been the irregularity of the fibers and of the locations of nucleosomes within them. Chromatin fibers have also been imaged in ice (14) and after low-temperature embedding (5) without revealing more than short stretches of the type of regularity predicted by model structures, making it unlikely that a failure of preparative methods to preserve an inherently symmetrical structure is involved. Recently, a thermodynamic argument favoring disorder in chromatin fibers has been advanced (15).

We have considered the structure of the native chromatin fiber in terms of two separate components: a level of DNA *folding* that is derived from the intrinsic properties of the nucleosome-linker unit and a degree of *compaction* determined by the local concentration of ions and other charged molecules. We discuss how folding may be affected by the variations in linker DNA length that occur in nature between consecutive nucleosomes (1, 16) and that will give rise to changes in the relative rotation angle as well as in the distance between them (17–19).

By separating folding from the more complex issue of compaction, we are able to avoid making assumptions that are implicit in most helical models but not well supported by experimental evidence. These include the imposition of symmetry via specific linker DNA trajectories and the involvement of specific nucleosome–nucleosome contacts in generating or maintaining periodicity in chromatin fibers. We show that structures derived using these minimal constraints share many of the features observed in chromatin.

MATERIALS AND METHODS

Model construction begins with a first nucleosome in an arbitrary orientation in three dimensional space (Fig. 1). The exiting linker continues in the plane established within the nucleosome, its trajectory in the plane being defined by the selected entry–exit angle (α). From the chosen linker length (L), defined here as the length of DNA in base pairs between chromatosomes (1), the coordinates of the linker entry point of nucleosome 2 are calculated. The plane of nucleosome 2 with respect to nucleosome 1 is established by the helical twist of DNA (selectable, and usually set at 10.4 bp per turn)

The publication costs of this article were defrayed in part by page charge payment. This article must therefore be hereby marked "*advertisement*" in accordance with 18 U.S.C. §1734 solely to indicate this fact.

†On leave from: Department of Molecular Biology, Moscow State University, Russia.

and L. We define the relative rotation between consecutive nucleosomes as the angle (β). The program includes the option of introducing the contribution of the chromatosome to the rotation angle. This requires selecting values for the average helical twist of the 146 bp of DNA on the nucleosome core and for the 20 bp of "chromatosome linker."

The coordinates of points along a helical ramp representing the DNA of nucleosome 2 are determined, after which the procedure repeats with the next linker. Nucleosome diameter and thickness are 11.0 nm and 5.5 nm, respectively (1), and the DNA rise per base pair is taken as 0.34 nm. From the linker entry/exit points, a histogram of the distance between nearest neighbors may be calculated, and a sliding average of the location of 10 or more nucleosomes is used to plot a "fiber" axis. The data may be displayed graphically as orthogonal projections or as three-dimensional perspective views that can be rotated interactively.

Long chromatin fibers were isolated in 80 mM monovalent ions from *Necturus maculosus* erythrocyte nuclei as described (10), fixed for 24 hr with 0.1% glutaraldehyde, adsorbed to carbon films in a thin layer of 5% glucose, and air dried. Chromatin fragments isolated from chicken erythrocyte nuclei were freeze-dried and shadowed as described (3). Sperm from the starfish *Patiria miniata* were homogenized briefly in artificial sea water, fixed in 2% glutaraldehyde in 150 mM NaCl/15 mM Hepes, pH 8.0, and embedded in Lowicryl K11M at −55°C, and thin sections were stained with osmium ammine B as described (20).

RESULTS

The nucleosome–linker system we have modeled is illustrated in Fig. 1. The entering and exiting linkers "cross" at the entry–exit site (21) where the globular domain of histone H1 is thought to be located and to "seal" the two turns of DNA (1). The rotation angle (β) between adjacent nucleosomes is determined by the length of the linker (L), which here represents the length of DNA between chromatosomes rather than nucleosomes. A complete turn of the double helix results in a 360° change in β. Changes in L also directly affect the spacing between adjacent nucleosomes. The only other variable in the model is the entry–exit angle (α) of the two linker DNAs. For chromatin in the uncompacted zig-zag conformation, observed under conditions least likely to affect this parameter, the angle is estimated to vary between 20 and 60 degrees (Fig. 4; ref. 22). Our algorithm allows variation of the number of base pairs of linker DNA between specified maxima and minima, either randomly or using a Gaussian distribution. In addition, the entry–exit angle (α) may be varied randomly over a specified range.

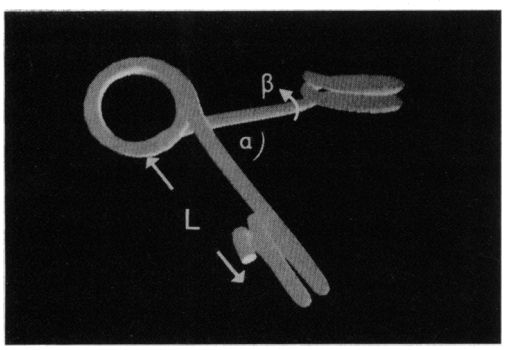

FIG. 1. The nucleosome–linker-nucleosome unit. α, Linker entry–exit angle; L, linker DNA length (distance between consecutive entry–exit points); β, rotation angle between consecutive nucleosomes.

Model Structures. We first determined the range of chromatin architectures defined by the model using fixed values for linker length and entry–exit angle. In all cases, a symmetrical linear assemblage of nucleosomes is produced, ranging from the completely extended beads-on-a-string (entry–exit angle, 180°) to fibers with densely packed nucleosomes. Some examples, covering a complete 360° "cycle" of rotation angles are shown in Fig. 2. Common features are helical arrangements of nucleosomes at the fiber periphery and an internal location of linker DNA. The latter property results in the dependence of diameter on linker length, a feature of two proposed models for the 30-nm chromatin fiber (9, 23).

Whereas the periodicity of the folding pattern is a general property of the nucleosome–linker unit, the precise location in the cycle for a given linker length is extremely sensitive to the value used for the helical twist of DNA. Also, the inclusion of a fixed contribution to β from the chromatosome (see *Materials and Methods*) has the effect of shifting the phase of the cycle different amounts depending on the values used for the twist of DNA on the nucleosome core and chromatosome portion of the linker. Given the present uncertainties in these values, it is not possible to assign with confidence the phase of cycle for a specific linker DNA length, and, as discussed below, an alternative empirical determination of β may be possible.

One parameter of isolated compact fibers that has been estimated from electric dichroism measurements is the tilt angle of the nucleosomal disk with respect to the fiber axis (24–26). In the modeled system, there is a simple linear relationship between β and nucleosome tilt, values of 0° (and 360°) for β resulting in nucleosomes oriented perpendicular to the fiber axis, whereas for $\beta = 180°$, the nucleosome disks are parallel to the axis (see Fig. 2). The reported values for

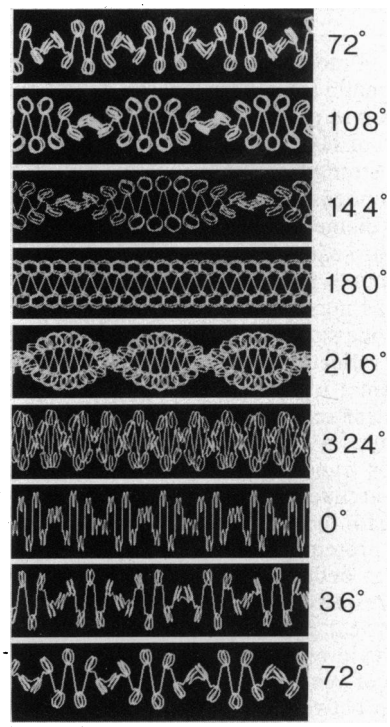

FIG. 2. Examples of the chromatin structures generated when linker DNA length between consecutive nucleosomes is kept constant (for a given run). At the right is shown the rotation angle between nucleosomes for each structure. For this series, linker DNA lengths (bp) were (from the top) 52, 53, 54, 55, 56, 59, 60, 61, and 62, the entry–exit angle (α) was 30° in all cases, and the DNA twist was 10 bp per turn. Structures with linker DNAs of 57 bp and 58 bp had high nucleosome packing ratios and are not illustrated.

nucleosome tilt (ranging from 30° to 45°) imply restrictions on allowable values for β. Nucleosome tilt is not affected by the linker entry–exit angle (α).

Effects of Varying Linker Length. Having established the basic architecture defined by the model, we investigated the effects of introducing progressively greater variability in the linker length between consecutive nucleosomes (Fig. 3). Starting with a fixed linker length (46 bp) producing a straight symmetrical fiber with circular cross section (Fig. 3*a*), the linker was allowed to vary from 45 to 47 bp (Fig. 3*b*), 44 to 48 bp (Fig. 3*c*), and 43 to 49 bp (Fig. 3*d*), in each case using a Gaussian distribution between the selected maxima and minima. The structures shown in Fig. 3 *b–d* are produced by a typical run of the program using the stated input parameters. In all cases, the fiber-like basic structure is maintained, but its three-dimensional trajectory is altered, at first producing a sinuous fiber in which the underlying symmetry of nucleosome positions is easily recognized (Fig. 3*b*). When the linker length is allowed to vary over 5 bp, abrupt changes in fiber trajectory are common, resulting in apparent discontinuities (Fig. 3*c*). However, short regions retaining some degree of visual order are still apparent. When the variation extends over 7 bp (mean ± 3 bp), the fiber follows a tortuous path (for clarity, only short 50-nucleosome stretches are shown in Fig. 3*d*) and nucleosome location appears to be completely disordered. Nevertheless, by interactively rotating such structures, it is possible to recognize short regions that retain some symmetry if viewed (or projected) in a specific direction. Throughout this range of variations, the mean fiber diameter remains remarkably constant. Variation of the linker entry–exit angle between selected maxima and minima also results in a loss of symmetry, but the effect is much smaller than that of linker length, while allowing variations in linker length and entry–exit angle has an additive effect (not shown).

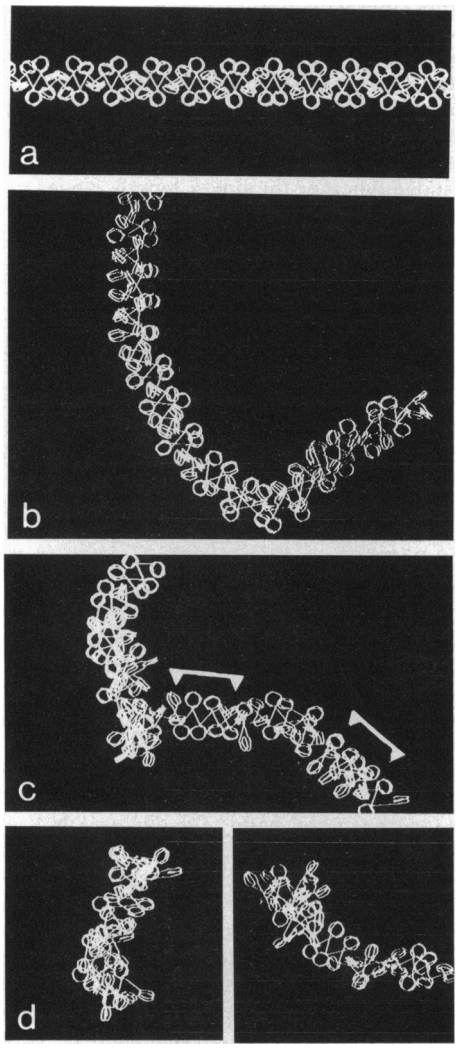

FIG. 3. Effect of introducing linker DNA length variability. (*a*) The initial conditions with fixed linker (46 bp) generate a symmetrical fiber. (*b*) By allowing the linker DNA to vary from 45 bp to 47 bp, a smoothly curving fiber is produced in which the symmetrical arrangement of nucleosomes is still apparent. (*c*) When the linker ranges from 44 bp to 48 bp, fibers show restricted regions where the nucleosome arrangement appears ordered (brackets) as well as sections with no apparent order. Abrupt changes in trajectory, apparent discontinuities, and local variations in fiber diameter are also obtained. (*d*) A much more disordered nucleosome arrangement is obtained when the linker varies from 43 bp to 49 bp. Despite the loss of symmetry, a fiber-like organization is retained, with mean diameter similar to that in *c* and *b*. A linker DNA twist of 10.4 bp per turn, nucleosomal DNA twist of 10.2 bp per turn (27), and entry–exit angle of 60° were used in all cases. For the fibers with varying linker, a Gaussian distribution of lengths based on a mean of 46 bp was used.

Comparison with Observed Chromatin Structures. Fig. 4 shows a fragment of isolated chicken erythrocyte chromatin prepared by freeze-drying, a technique that avoids the flattening effect of surface forces. To the right, is a group of six individual nucleosomes in which the linker DNA elements are mostly straight. Two of the nucleosomes (identified by arrowheads) are seen "edge on" rather than flat on the substrate. This effect, recently confirmed by imaging oligonucleosomes suspended in vitreous ice (C.L.W., J. Bednar, and J. Dubochet, unpublished results), suggests that consecutive nucleosomes are rotated a significant amount with respect to each other.

Normally, it is not possible to resolve nucleosomes and linker DNA in thin sections of nuclei. However, low-temperature embedding (5), in conjunction with a DNA-specific stain (20) and observation at low temperature, provides significant improvement. Fig. 5 shows selected regions of chromatin fiber in thin sections of starfish sperm nuclei fixed in 150 mM NaCl. These nuclei have a normal complement of histones and typical nucleosomal organization (28). In some places, the clearly defined nucleosomes (small arrowheads) are connected by thin filaments (large arrowheads), suggesting that at least some linker DNA is extended *in situ*.

A striking effect of introducing linker variability to the model structures is the complex trajectories that are generated (Fig. 3 *b* and *c*). Similar conformations are observed if isolated chromatin fibers, fixed in 80 mM NaCl, are embedded unstained in a thin film of glucose (Fig. 6).

Under these conditions, designed to preserve the overall shape and mass density of the fibers, smooth and abrupt changes in fiber direction are seen, as well as apparent discontinuities. The diameter and mass density of the fibers

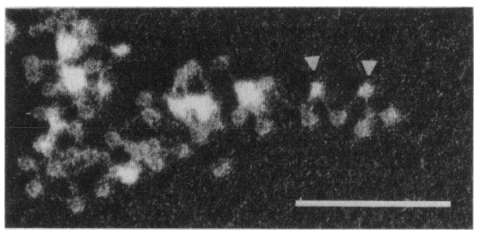

FIG. 4. Isolated polynucleosome from chicken erythrocyte nucleus after freeze-drying and light shadowing. At the right is a group of six consecutive nucleosomes in which the linker DNA segments are almost straight. Some nucleosomes have adhered *en face* to the carbon film whereas others (arrowheads) appear more edge on. (Bar = 100 nm.)

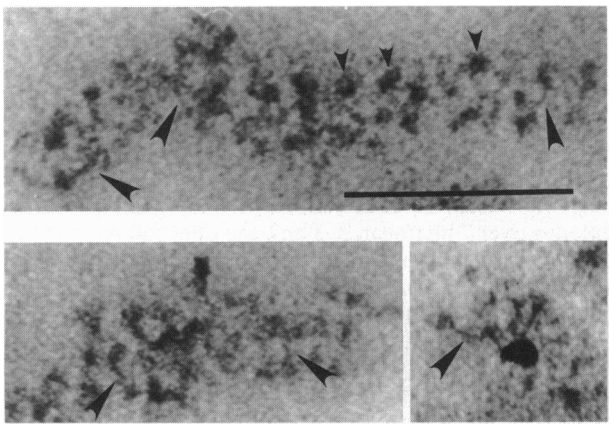

FIG. 5. Selected fibers from a thin section of a starfish sperm nucleus stained with the osmium ammine B reagent. The chromatin fibers show clearly defined nucleosomes (small arrowheads) that are in some cases interconnected by filaments of extended linker DNA (large arrowheads) that have a maximum length of ≈20 nm. The dark spot at the bottom right is a gold particle on the surface of the section. (Bar = 100 nm.)

also show the type of short-range variation seen in the model structures of Fig. 3 *c* and *d*. Three-dimensional reconstructions of chromatin fibers *in situ* also show similar complex trajectories and local variations in diameter and density (29).

DISCUSSION

Our strategy for predicting chromatin folding patterns produces structures that mimic many of the features observed in isolated and *in situ* chromatin fibers. In establishing the initial conditions, we assume no inherent symmetry or specific nucleosome–nucleosome interactions but use only properties of the nucleosome–linker unit under conditions of minimal salt-induced compaction. An extended linker DNA is observed under such conditions (Fig. 4; ref. 2), and although persistence length effects will produce some deviation from the straight linker segments generated by the model, for such short DNA lengths (19) this will produce only a small additional (and random) variability in the final structures.

The most interesting feature of the model structures obtained when the linker length is varied (Fig. 3) is the degree

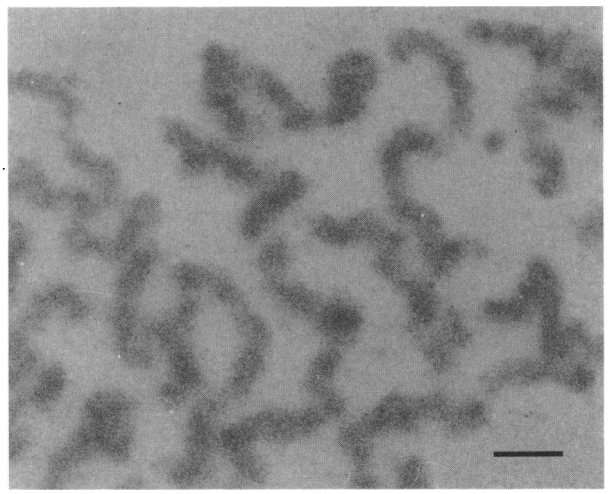

FIG. 6. Isolated polynucleosomes from *N. maculosus* erythrocytes prepared and fixed in 80 mM monovalent ions and embedded unstained in a thin film of neutral glucose. The chromatin fibers show the type of morphology obtained by introducing linker DNA variability of 3–7 bp in model structures (see Fig. 3). (Bar = 100 nm.)

to which they resemble actual chromatin fibers. By allowing one parameter, linker length, to vary, chromatin structures are obtained that (*i*) occupy approximately cylindrical volumes with mean diameters similar to those of chromatin fibers, (*ii*) follow complex three-dimensional trajectories, (*iii*) show regions in which there is local short-range periodicity in nucleosome position, and (*iv*) have nucleosomes positioned toward the periphery of the fiber.

Structures bearing a close resemblance to chromatin fibers are obtained with linker variations of ±2 bp and ±3 bp (Fig. 3), values considerably lower than the mean ± 17 bp reported for trimmed di- and trinucleosomes from rat liver (ref. 16; see also discussion in ref. 14). However, within populations of trimmed dinucleosomes, quantization of linker lengths at ≈10-bp intervals was found (18), implying a conservation of nucleosome rotational setting, and a similar conclusion was reached from DNase I digestion studies (17). Quantization of mean nucleosome spacing among eukaryotes in general has also been discussed (19), and the possibility has been raised that short-range nucleosome spacings may be quite regular (30). More information concerning local translational and rotational settings of consecutive nucleosomes is required in order to judge whether the linker length ranges used in Fig. 4 are representative of the *in vivo* state.

Chromatin Compaction. Our model system predicts the folding geometry of the nucleosome–linker unit and does not address the changes that are known to occur *in vitro* as a function of the salt concentration of the medium. The salt-induced transitions of chromatin *in vitro* have been extensively studied and analyzed in terms of the effects of charge shielding and neutralization on the mutual repulsion of DNA (e.g., ref. 31).

In considering an extension of the folding model to salt-compacted chromatin, it is important to know whether the conformation of the linker DNA changes during the compaction process. At present, the data on this issue are conflicting. UV-induced thymine dimers occur preferentially in bent DNA and are largely confined to nucleosomal rather than linker DNA in intact nuclei (32, 33). Measurements of parameters such as x-ray scattering (34) and polarized photobleaching (35) provide no evidence of the changes expected for a transition from a straight to a curved linker as the extended chain of nucleosomes folds into a compact fiber. Also, thin sections of chromatin fibers fixed *in situ*, and stained with the DNA-specific osmium ammine B reagent, show filaments that are most likely extended linker DNA (Fig. 5). On the other hand, the linker DNA of isolated dinucleosomes does show H1-independent salt-induced bending, allowing the two nucleosomes to touch (36, 37), but not to assume the face-to-face contact expected in a solenoidal fiber. Also, reconstituted nucleosome 12-mers undergo a salt-induced compaction independent of histone H1 and thought to involve the bending of linker DNA (38).

Thus, the principal evidence that linker DNA bends during salt-induced compaction is derived from *in vitro* studies, whereas evidence to the contrary has been obtained from chromatin in the nucleus. Certainly, changes in chromatin compaction appear to occur *in vivo* as well as *in vitro*, and, if the basic folding of the nucleosomal chain occurs as suggested here, then compaction must entail either a bending of linker DNA or a change in linker entry–exit angle or both. Such changes in linker conformation could be limited to that needed to condense the fiber, rather than involve the supercoiling required to bring neighboring nucleosomes together in a solenoidal configuration.

Tests and Applications. In principle, the folding model discussed here may be tested by observing the orientations of nucleosomes on chromatin with mapped nucleosome locations (39, 40). Recently, the technical feasibility of making measurements of this sort has been demonstrated by the

three-dimensional reconstruction of individual DNA molecules in the native fully hydrated state (41). The application of this approach to defined chromatin structures will enable the predictions of our folding proposal to be tested. It should also be possible from such studies to determine directly the relative rotation of the DNA between the entry and exit sites on a nucleosome [perhaps variable, and dependent on the sequence of nucleosomal DNA (42)], the range of linker DNA entry–exit angles, and the changes that occur during the early stages of salt-induced compaction.

We thank J. Bednar and P. Furrer for assistance with modeling Fig. 1 and L. S. Jarrett for assistance with Fig. 4. This research was supported by National Institutes of Health Grant GM43786 to C.L.W. The Microscopy and Imaging Facility (University of Massachusetts, Amherst) is supported in part by National Science Foundation Grant BBS 87-14235.

1. van Holde, K. E. (1988) *Chromatin* (Springer, New York).
2. Thoma, F., Koller, T. & Klug, A. (1979) *J. Cell Biol.* **83,** 403–427.
3. Woodcock, C. L. F., Frado, L.-L. Y. & Rattner, J. B. (1984) *J. Cell Biol.* **99,** 42–52.
4. Davies, H. G., Murray, A. B. & Walmsley, M. E. (1974) *J. Cell Sci.* **16,** 261–299.
5. Horowitz, R. A., Giannasca, P. J. & Woodcock, C. L. (1990) *J. Microsc.* **157,** 205–224.
6. Langmore, J. P. & Paulson, J. R. (1983) *J. Cell Biol.* **96,** 1120–1131.
7. Felsenfeld, G. & McGhee, J. D. (1986) *Cell* **44,** 375–377.
8. Rattner, J. B. & Hamkalo, B. A. (1978) *Chromosoma* **69,** 363–379.
9. Williams, S. P., Athey, B. D., Muglia, L. J., Schappe, R. S., Gough, A. H. & Langmore, J. P. (1986) *Biophys. J.* **49,** 233–248.
10. Woodcock, C. L., Woodcock, H. & Horowitz, R. A. (1991) *J. Cell Sci.* **99,** 99–106.
11. Woodcock, C. L., McEwen, B. F. & Frank, J. (1991) *J. Cell Sci.* **99,** 107–114.
12. Ris, H. & Kubai, D. F. (1970) *Annu. Rev. Genet.* **4,** 263–294.
13. Woodcock, C. L. (1992) in *Electron Tomography*, ed. Frank, J. (Plenum, New York), pp. 281–312.
14. Athey, B. D., Smith, M. F., Williams, S. P., Rankert, D. A. & Langmore, J. P. (1990) *J. Cell Biol.* **111,** 795–806.
15. Subirana, J. A. (1992) *FEBS Lett.* **302,** 105–107.
16. Strauss, F. & Prunell, A. (1982) *Nucleic Acids Res.* **10,** 2275–2293.
17. Lohr, D. & van Holde, K. E. (1979) *Proc. Natl. Acad. Sci. USA* **76,** 6326–6330.
18. Strauss, F. & Prunell, A. (1983) *EMBO J.* **2,** 51–56.
19. Widom, J. (1992) *Proc. Natl. Acad. Sci. USA* **89,** 1095–1099.
20. Horowitz, R. A. & Woodcock, C. L. (1992) *J. Histochem. Cytochem.* **40,** 123–133.
21. Zivanovic, Y., Duband-Goulet, I., Schultz, P., Stofer, E., Oudet, P. & Prunell, A. (1990) *J. Mol. Biol.* **214,** 479–495.
22. Dubochet, J., Adrian, M., Chang, J.-J., Homo, J.-C., Lepault, J., McDowall, A. W. & Schultz, P. (1988) *Q. Rev. Biophys.* **21,** 129–288.
23. Bordas, J., Perez-Grau, L., Koch, M. H. J., Vega, M. C. & Nave, C. (1986) *Eur. Biophys. J.* **13,** 175–185.
24. McGhee, J. D., Nickol, J. M., Felsenfeld, G. & Rau, D. C. (1983) *Cell* **33,** 831–841.
25. Mitra, S., Sen, D. & Crothers, D. M. (1984) *Nature (London)* **308,** 247–250.
26. Sen, D., Mitra, S. & Crothers, D. M. (1986) *Biochemistry* **25,** 3441–3447.
27. Drew, H. R. & Travers, A. A. (1985) *J. Mol. Biol.* **186,** 773–790.
28. Giannasca, P. J., Horowitz, R. A. & Woodcock, C. L. (1993) *J. Cell Sci.* **105,** 551–561.
29. Woodcock, C. L., Horowitz, R. A. & Agard, D. A. (1992) in *Proceedings of the 50th Annual Meeting of the Electron Microscopy Society of America*, eds. Bailey, G. W., Bentley, J. & Small, J. A. (San Francisco Press, San Francisco), pp. 498–499.
30. Lauderdale, J. D. & Stein, A. (1993) *Biochemistry* **32,** 489–499.
31. Clark, D. J. & Kimura, T. (1990) *J. Mol. Biol.* **211,** 883–896.
32. Pehrson, J. R. (1989) *Proc. Natl. Acad. Sci. USA* **86,** 9149–9153.
33. Pehrson, J. R. & Cohen, L. (1992) *Nucleic Acids Res.* **20,** 1321–1324.
34. Greulich, K. O., Wachtel, E., Ausio, J., Seger, D. & Eisenberg, H. (1987) *J. Mol. Biol.* **193,** 709–721.
35. Selvin, P. R., Scalettar, B. A., Langmore, J. P., Axelrod, D. & Hearst, J. E. (1990) *J. Mol. Biol.* **214,** 377–390.
36. Yao, J., Lowary, P. T. & Widom, J. (1990) *Proc. Natl. Acad. Sci. USA* **87,** 7603–7607.
37. Yao, J., Lowary, P. T. & Widom, J. (1991) *Biochemistry* **30,** 8408–8414.
38. Garcia-Ramirez, M., Dong, F. & Ausio, J. (1992) *J. Biol. Chem.* **267,** 19587–19595.
39. Thoma, F. (1992) *Biochim. Biophys. Acta* **1130,** 1–19.
40. Simpson, R. T. (1991) *Prog. Nucleic Acid Res. Mol. Biol.* **40,** 143–184.
41. Dustin, I., Furrer, P., Stasiak, A., Dubochet, J., Langowski, J. & Egelman, E. (1991) *J. Struct. Biol.* **107,** 15–21.
42. Shimizu, M., Roth, S. Y., Szent-Gyorgi, C. & Simpson, R. T. (1991) *EMBO J.* **10,** 3033–3041.